G. Carta et alii, Frattura ed Integrità Strutturale, 29 (2014) 28-36; DOI: 10.3221/IGF-ESIS.29.04

Focussed on: Computational Mechanics and Mechanics of Materials in Italy

Elastic wave propagation and stop-band generation in strongly damaged solids

G. Carta, M. Brun
Department of Mechanical, Chemical and Materials Engineering, University of Cagliari, Italy
giorgio_carta@unica.it, mbrun@unica.it

A.B. Movchan
Department of Mathematical Sciences, University of Liverpool, UK
abm@liverpool.ac.uk

ABSTRACT. In this work, we study the propagation of elastic waves in elongated solids with an array of equally-spaced deep transverse cracks, focusing in particular on the determination of stop-bands. We consider solids with different types of boundary conditions and different lengths, and we show that the eigenfrequencies associated with non-localized modes lie within the pass-bands of the corresponding infinite periodic system, provided that the solids are long enough. In the stop-bands, instead, eigenfrequencies relative to localized modes may be found. Furthermore, we use an asymptotic reduced model, whereby the cracked solid is approximated by a beam with elastic connections. This model allows to derive the dynamic properties of damaged solids through analytical methods. By comparing the theoretical dispersion curves yielded by the asymptotic reduced model with the numerical outcomes obtained from finite element computations, we observe that the asymptotic reduced model provides a better fit to the numerical data as the slenderness ratio increases. Finally, we illustrate how the limits of the stop-bands vary with the depth of the cracks.

KEYWORDS. Elastic waves; Dispersion; Stop-bands; Elastic solids; Cracks; Asymptotics.

INTRODUCTION

Discontinuities in elastic solids give rise to stop-bands, which are intervals of frequencies for which waves travelling through the solid are attenuated in amplitude, also if damping is absent. Examples of discontinuities are cracks, imperfections and defects. In addition, discontinuities may be represented by non-smooth reductions of cross-sections due to design purposes. For instance, long bridges consisting of several spans that are simply-supported on piers usually present narrower cross-sections in correspondence of the piers, where the spans are connected only by the upper deck.

The generation of stop-bands is generally accompanied by localization phenomena, such as trapped modes occurring near discontinuities. Localization has been observed in different elastic systems, like beams [1], plates [2] and micro-structured media [3-5]. Localization around defects in bi-material delaminating systems is investigated in [6,7], where a lower-dimensional asymptotic model is introduced to study the dispersion properties of the medium. An improved formulation

with higher-order terms in the asymptotic approximation of the system is proposed in [8] for the analysis of Floquet-Bloch waves.
An elongated elastic solid with a deep transverse crack is examined in [9,10] for the cases of static longitudinal and transverse loads, respectively. In [9,10] a reduced model is formulated, in which the cracked region is approximated asymptotically by an elastic connection, which accounts for the decay of the boundary layer arising near the crack. This model is extended in [11] to dynamic problems.
The presence of a crack influences the vibration response of a beam, since it locally modifies the flexibility of the structural element [12]. In [13] the effects of both a double-sided and a single-sided crack on the natural frequencies of a cantilever beam are investigated. In [14] the changes in the lowest eigenfrequency of a simply-supported beam produced by a breathing edge crack are discussed in comparison with experimental results.
In this paper, we analyze the dynamic response of an elongated elastic solid with a distributed damage, represented by equally-spaced transverse cracks. First, we determine numerically the eigenfrequencies and eigenmodes of cracked solids with different boundary conditions and different lengths, and we compare the results with the dispersion curves computed for solids with infinite length. Successively, we assess the validity of the reduced asymptotic model examined in [11] for different values of the slenderness ratio of the solid, and we evaluate the positions of the stop-bands in relation with the depth of the cracked sections. Finally, we summarize the results and we discuss briefly the practical applications that can be related to this work.

DYNAMIC PROPERTIES OF ELONGATED DAMAGED SOLIDS WITH DIFFERENT BOUNDARY CONDITIONS

We examine the dynamic behavior of an elongated elastic solid with equally-spaced cracks. An example of such a solid with a rectangular cross-section and simply-supported conditions is drawn in Fig. 1a, where l is the distance between cracks, while L, h and b are the length, the height and the thickness of the solid, respectively. Since the distance between cracks is constant, the solid can be modeled as a sequence of repetitive cells, one of which is shown in Fig. 1b, where s denotes the height of the cracked section.

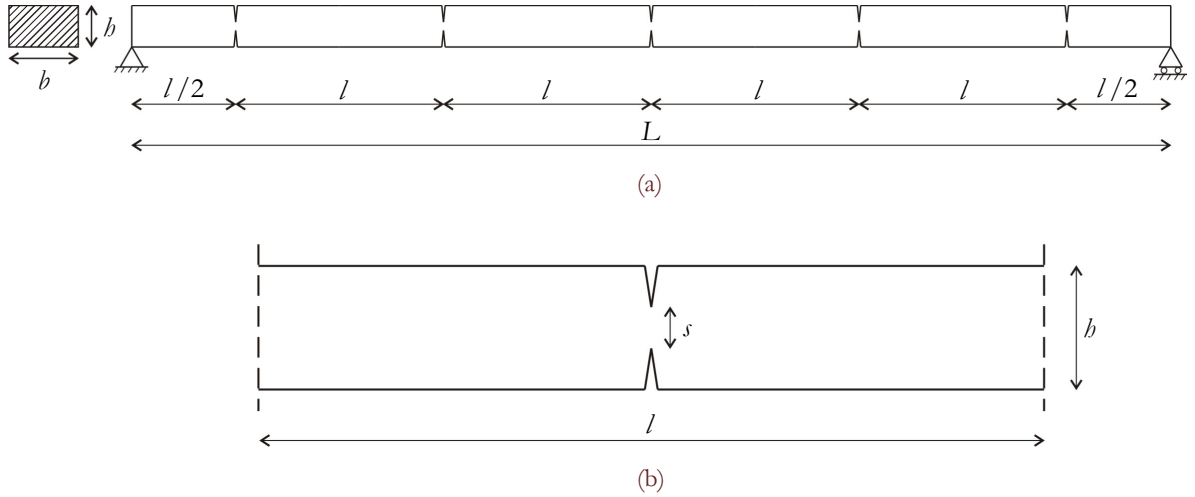

Figure 1: (a) Simply-supported elongated solid with cracks located at regular intervals of length l; (b) repetitive cell of the solid.

We consider time-harmonic waves propagating along the axis of the solid that consist of oscillations occurring in the direction of the solid height. This assumption allows to study the solid as a two-dimensional strip subjected to transverse oscillations.
By using a finite element model developed in the software *Comsol Multiphysics*, we obtain the eigenfrequencies and eigenmodes of damaged solids with different lengths. In Figs. 2a-2e we report the results relative to five different boundary conditions: a hinge and a roller, both ends fixed, a fixed end and a roller, a slider and a roller, a slider and a fixed end. The parameter n in the horizontal axes stands for the number of repetitive cells, while the quantity ϕ in the vertical axes is a non-dimensional frequency given by $\phi = (\varrho A \omega^2 l^4 / EJ)^{1/4}$.

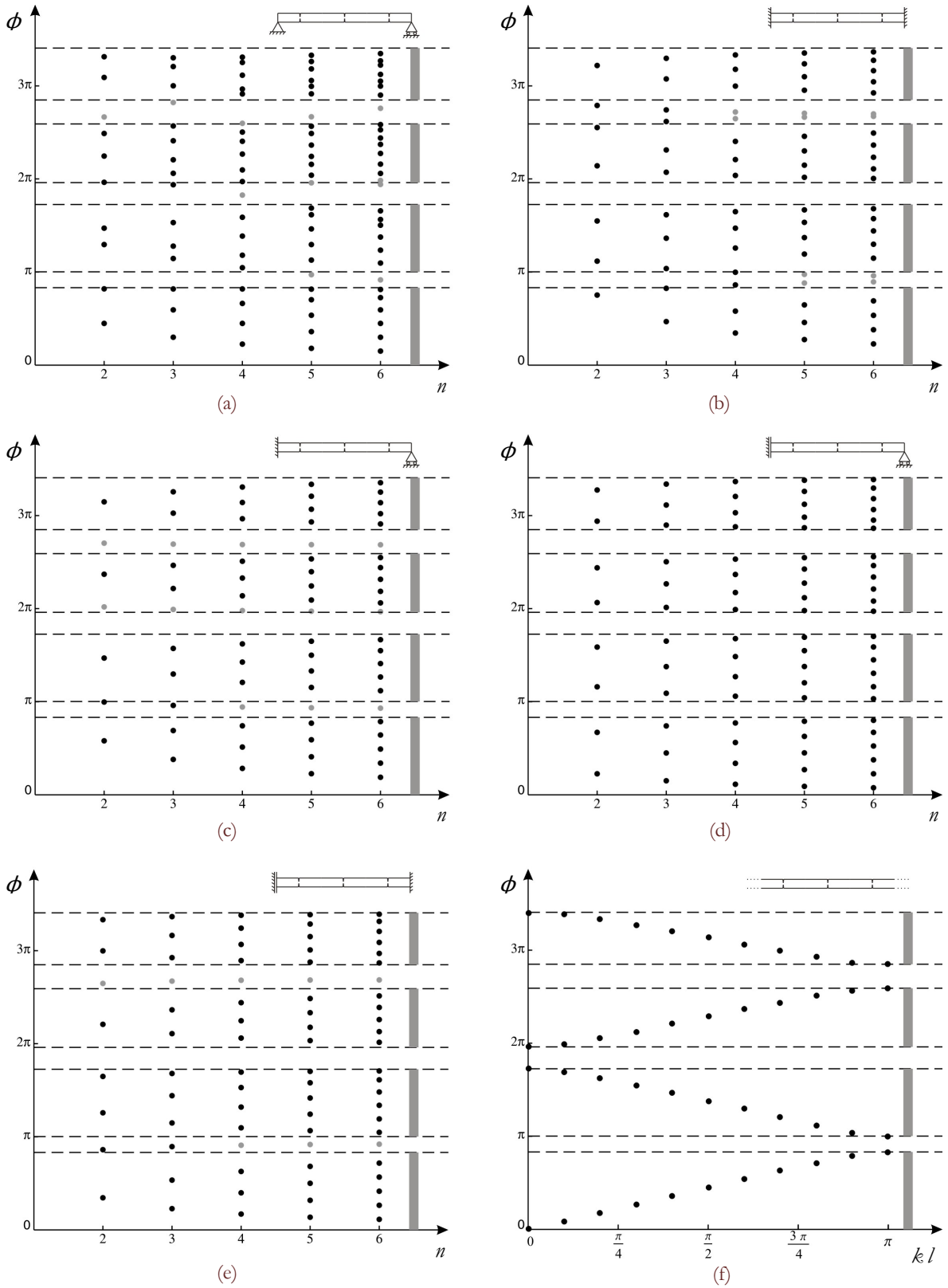

Figure 2: (a)-(e) Eigenfrequencies of cracked solids with different lengths and different boundary conditions, sketched at the top-right corner of each figure; (f) dispersion curves (black dots) and pass-bands (grey lines) for the solid with infinite length.

In this paper, E is the Young's modulus, ν is the Poisson's ratio, ϱ is the mass density, ω is the angular frequency, while A and J are the area and the second moment of inertia of the cross-section of the solid. The results in Figs. 2a-2e are determined by assigning the following properties to the solid: E = 31 GPa, ν = 0.2, ϱ = 2500 kg/m^3, l = 3 m, h = 0.3 m, s = 0.1 m, b = 0.5 m. The black dots indicate the eigenfrequencies associated with propagating modes, while the grey dots represent the eigenfrequencies corresponding to localized modes. Examples of propagating and localized modes for the different cases are shown in Fig. 3. We point out that the solid with a slider and a roller does not exhibit localized modes (see Fig. 2d).

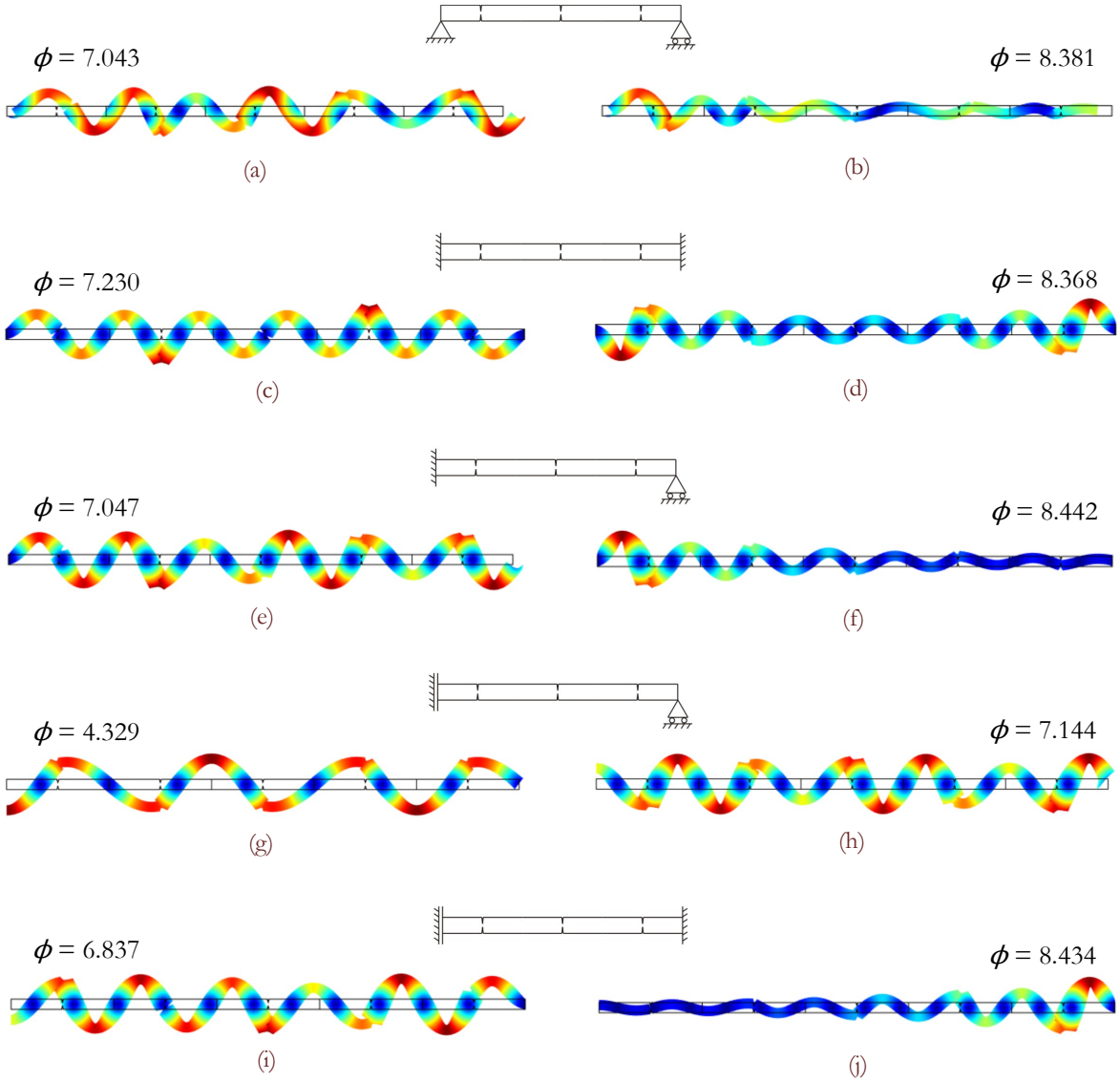

Figure 3: Examples of propagating eigenmodes ((a), (c), (e), (g), (h), (i)) and localized eigenmodes ((b), (d), (f), (j)) of solids with n = 5 repetitive cells and with different boundary conditions, shown in the insets.

The dispersion curves for an infinite cracked solid are shown in Fig. 2f, where k is the wavenumber. The dispersion curves are obtained from a finite element model in *Comsol Multiphysics* by imposing Floquet-Bloch conditions at the vertical sides of the repetitive cell in Fig. 1b. The frequency ranges for which waves propagate without attenuation are denoted by "pass-bands" and are illustrated in grey color on the right of Figs. 2a-2f. On the other hand, the frequency ranges for which waves decay exponentially are called "stop-bands".
From the outcomes in Fig. 2 we infer that the majority of the eigenfrequencies associated with propagating modes fall inside the pass-bands, while most of the eigenfrequencies relative to localized modes lie within the stop-bands.

Nonetheless, there are some exceptions: especially for short solids, namely for low values of n, some eigenfrequencies corresponding to propagating modes are found outside the pass-bands, though close to their limits; however, these modes tend to become localized as the length of the solid or, equivalently, n is increased. Therefore, the effect of periodicity is more evident in long solids, as could be predicted. The results discussed above are in agreement with those presented in [15] for mono-coupled systems, in [11] for a strip made of steel with free ends, and in [16] for a real bridge.

ASSESSMENT OF AN ASYMPTOTIC REDUCED MODEL FOR THE DYNAMIC STUDY OF ELONGATED SOLIDS

The analytical determination of the dynamic properties of cracked solids modeled as two-dimensional or three-dimensional continuous media is not a straightforward task. Therefore, simpler analytical models have been proposed in the literature. In particular, we investigate the "asymptotic reduced model", firstly formulated in [10] for static problems and later extended in [11] to dynamic problems. This model is defined as "reduced" because it approximates the elongated strip in Fig. 1 as a beam, in which the cracked sections are treated as elastic connections consisting of rotational and translational springs. The stiffnesses of these springs are evaluated via asymptotic techniques [10,11,17], which explains the use of the adjective "asymptotic" appended to the definition of the model in exam.
In this work, we assess the validity of the asymptotic reduced model for different values of the "slenderness ratio" l/h. We consider both cracked and undamaged solids, and we compute the dispersion curves of the corresponding beam models.
In order to obtain the dispersion curves for a beam with elastic connections, we consider an infinite periodic beam made of repetitive cells, as that drawn in Fig. 4. Here, K_b and K_s are the rotational (or bending) and translational (or shear) stiffnesses of the springs that simulate the cracked sections of the solid. They are expressed by [10,11]

$$K_b = \frac{\pi E b s^2}{4(5-2\nu)(1+\nu)} \tag{1}$$

and

$$K_s = \frac{\pi E b}{4(1-\nu^2)\log(h/s)} \tag{2}$$

respectively. All the quantities appearing in the formulae above have been defined in the previous section.

We derive the dispersion curves by using the method based on the transfer matrix [18-21]. The transfer matrix links the generalized displacements and forces at the two ends of the repetitive cell of a periodic structure. For the case at hand, the transfer matrix is given by [11]

$$\mathbf{T} = \begin{bmatrix} \frac{\cos(\phi)+\cosh(\phi)}{2} & \frac{\sin(\phi)+\sinh(\phi)}{2\beta} & \frac{\cos(\phi)-\cosh(\phi)}{2\beta^2 EJ} & \frac{\sin(\phi)-\sinh(\phi)}{2\beta^3 EJ}+\frac{1}{K_s} \\ \frac{-\beta[\sin(\phi)-\sinh(\phi)]}{2} & \frac{\cos(\phi)+\cosh(\phi)}{2} & \frac{-\sin(\phi)-\sinh(\phi)}{2\beta EJ}-\frac{1}{K_b} & \frac{\cos(\phi)-\cosh(\phi)}{2\beta^2 EJ} \\ \frac{\beta^2 EJ[\cos(\phi)-\cosh(\phi)]}{2} & \frac{\beta EJ[\sin(\phi)-\sinh(\phi)]}{2} & \frac{\cos(\phi)+\cosh(\phi)}{2} & \frac{\sin(\phi)+\sinh(\phi)}{2\beta} \\ \frac{-\beta^3 EJ[\sin(\phi)+\sinh(\phi)]}{2} & \frac{\beta^2 EJ[\cos(\phi)-\cosh(\phi)]}{2} & \frac{-\beta[\sin(\phi)-\sinh(\phi)]}{2} & \frac{\cos(\phi)+\cosh(\phi)}{2} \end{bmatrix} \tag{3}$$

where $\beta = \phi/l$. Floquet-Bloch conditions lead to the following equation:

$$\det\left(\mathbf{T} - e^{ikl}\,\mathbf{I}\right) = 0 \tag{4}$$

where $\mathbf{I}$ is the identity matrix. Eq. (4) represents the dispersion relation for the beam with elastic connections. It can also be applied to an undamaged beam by taking $K_b \to \infty$ and $K_s \to \infty$.

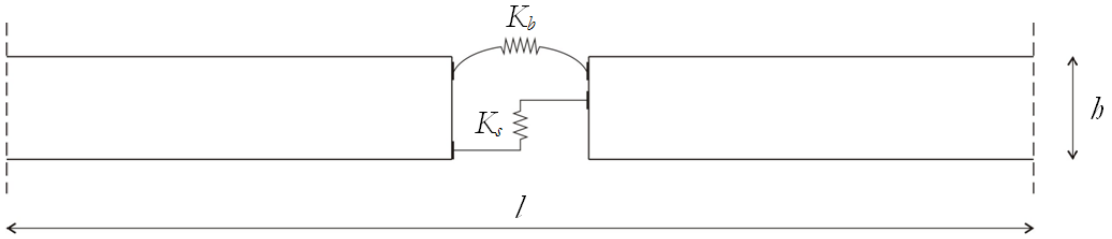

Figure 4: Repetitive cell of an infinite periodic beam with elastic connections.

We plot the analytical results in Fig. 5 in solid lines. Figs. 5a, 5c and 5e contain the dispersion curves for cracked beams, while Figs. 5b, 5d and 5f show the dispersion curves for undamaged beams. Three different values of slenderness ratio are considered: $l/h = 5$ (Figs. 5a and 5b), $l/h = 10$ (Figs. 5c and 5d) and $l/h = 20$ (Figs. 5e and 5f). The dots represent instead the numerical outcomes relative to strips having the same properties as the beams, which are derived from finite element computations. In particular, the numerical results in Fig. 5c are identical to those reported in Fig. 2f.

The diagrams in Fig. 5 show that the range of validity of the asymptotic reduced model increases with the slenderness of the solid. More specifically, for $l/h = 5$ only the first dispersion curve for the solid (either cracked or undamaged) is predicted well by the beam model; for $l/h = 10$, the first two theoretical dispersion curves determined with the asymptotic reduced model fit well the numerical data computed for the solid; for $l/h = 20$, the effectiveness of the beam model extends to the first four dispersion curves.

As shown in [11], the limits of the stop-bands coincide with the eigenfrequencies of the simple beams sketched at the bottom-right corners of Figs. 6a-6d. Therefore, simple analytical expressions can be used to determine the limits of the pass (propagation) and stop (non propagation) bands. The positions of the stop-bands along the frequency axis depend on the stiffnesses of the elastic junctions K_b and K_s. For the case of beams with rectangular cross-sections, K_b and K_s can be expressed in normalized form as functions of the slenderness ratio l/h, the "integrity ratio" s/h and the Poisson's ratio ν, as follows:

$$\kappa_b = \frac{K_b l}{EJ} = \frac{3\pi}{(5-2\nu)(1+\nu)} \frac{l}{h}\left(\frac{s}{h}\right)^2 \tag{5}$$

$$\kappa_s = \frac{K_s l^3}{EJ} = \frac{3\pi}{1-\nu^2}\left(\frac{l}{h}\right)^3 \frac{1}{\log(h/s)} \tag{6}$$

In the formulae above, κ_b and κ_s are the normalized bending and shear stiffnesses, respectively. In Figs. 6a-6d, we illustrate the relations between the first normalized eigenfrequencies ϕ_1 of the four simple beams shown in the figures and the integrity ratio s/h, for given values of the slenderness ratio and Poisson's ratio. The diagrams in Figs. 6a-6d are obtained, respectively, from the following approximate formulae [11], after substituting the expressions of κ_b and κ_s given by Eqs. (5) and (6):

$$\phi_1 = 2\sqrt[4]{6\frac{\kappa_b}{2+\kappa_b}} \tag{7}$$

$$\phi_1 = 2\sqrt[4]{6\frac{840+35\kappa_s-\sqrt{105}\sqrt{6720+336\kappa_s+11\kappa_s^2}}{336+\kappa_s}} \tag{8}$$

$$\phi_1 = 2\sqrt{3}\sqrt[4]{10\frac{21+7\kappa_b-\sqrt{7}\sqrt{53+30\kappa_b+5\kappa_b^2}}{5+\kappa_b}} \tag{9}$$

$$\phi_1 = 2\sqrt{3}\sqrt[4]{10\frac{840+7\kappa_s-\sqrt{35}\sqrt{20160+48\kappa_s+\kappa_s^2}}{720+\kappa_s}} \tag{10}$$

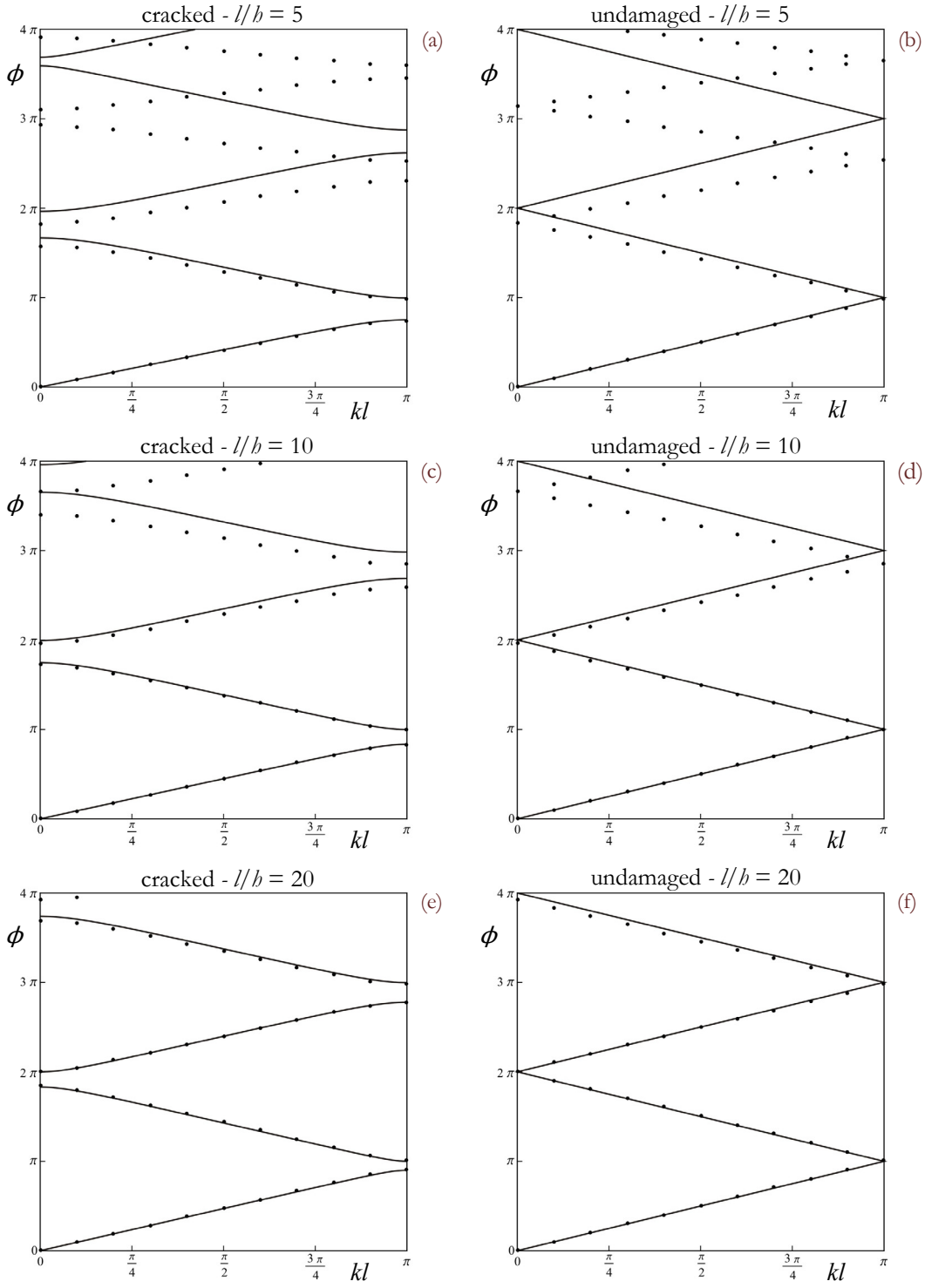

Figure 5: Theoretical (solid lines) and numerical (dots) dispersion curves for cracked and undamaged solids with $l = 1.5$ m ((a), (b)), $l = 3$ m ((c), (d)) and $l = 6$ m ((e), (f)). The other quantities have the following values: $h = 0.3$ m, $s = 0.1$ m, $b = 0.5$ m, $E = 31$ GPa, $\nu = 0.2$, $\varrho = 2500$ kg/m^3.

The diagrams in Figs. 6a and 6b represent the limits of the first stop-band, while the curves in Figs. 6c and 6d describe the limits of the second stop-band. We note that the lower limits of the first stop-band (Fig. 6a) and of the second stop-band (Fig. 6c) change significantly with s/h; on the other hand, the upper limits of the first stop-band (Fig. 6b) and of the second stop-band (Fig. 6d) are almost constant. Therefore, the main effect of the cracks is to open stop-bands in correspondence of the values that the dispersion curves for undamaged beams assume at $kl = 0$ and $kl = \pi$ (see Fig. 5d), keep the upper limits of the stop-bands almost constant and shift downwards the lower limits by an amount proportional to the depth of the crack.

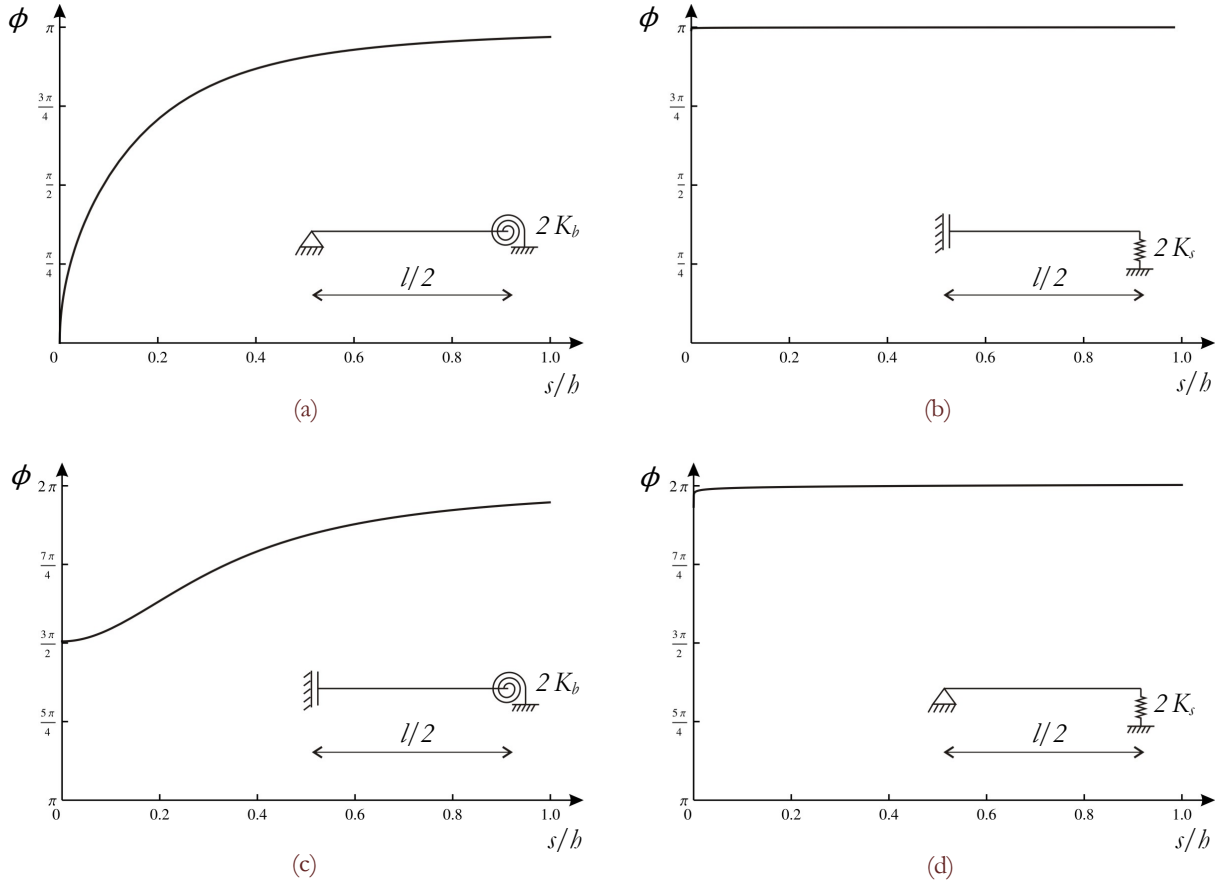

Figure 6: First eigenfrequencies versus integrity ratio s/h of simple beams with different boundary conditions, defining the limits of the stop-bands predicted by the beam model ($l/h = 10$, $\nu = 0.2$).

CONCLUSIONS

In this paper, we have examined the dynamic properties of elongated elastic solids with a distributed damage, studied as two-dimensional strips with equally-spaced cracks. By performing finite element simulations, we have found that the eigenfrequencies of long finite strips corresponding to propagating modes fall inside the pass-bands of infinite strips with the same properties, for any boundary conditions imposed at the ends. On the other hand, the eigefrequencies associated with localized modes are found in the stop-bands. The above considerations apply also to shorter strips, though in this case some exceptions are observed.

Successively, we have tested the effectiveness of an asymptotic reduced model, which approximates the cracked solid as a beam with elastic connections. This model allows to evaluate analytically the dynamic properties of the cracked solid. We have demonstrated that the validity of the model is enhanced as the slenderness of the beam is increased. In addition, we have provided the explicit expressions of the limits of the first two stop-bands as functions of the ratio between the heights of the cracked and undamaged sections of the beam.

The results of this work can be used in the context of Structural Health Monitoring for the detection of cracks, defects and imperfections in structural elements. Moreover, they can be exploited to design filtering systems with appropriate discontinuities that can stop the transmission of waves of specified frequencies.
It remains a big challenge to study analytically the dynamic properties of solids with randomly-distributed cracks or defects.

REFERENCES

[1] Movchan, A.B., Slepyan, L.I., Band gap Green's functions and localized oscillations, Proc. R. Soc. A, 463 (2007) 2709-2727.
[2] Poulton, C.G., Movchan, A.B., Movchan, N.V., McPhedran, R.C., Analytic theory of defects in periodically structured elastic plates, Proc. R. Soc. A, 468 (2012) 1196-1216.
[3] Mishuris, G.S., Movchan, A.B., Slepyan, L.I., Localization and dynamic defects in lattice structures, in: V.V. Silberschmidt (Ed.), Computational and experimental mechanics of advanced materials (CISM Courses and Lectures), Vol. 514, Springer, Wien, (2009) 51-82.
[4] Bigoni, D., Guenneau, S., Movchan, A.B., Brun, M., Elastic metamaterials with inertial locally resonant structures: application to lensing and localization, Phys. Rev. B, 87 (2013) 174303.
[5] Carta, G., Jones, I.S., Brun, M., Movchan, N.V., Movchan, A.B., Crack propagation induced by thermal shocks in structured media, Int. J. Solids Struct., 50 (2013) 2725-2736.
[6] Mishuris, G.S., Movchan, A.B., Bercial, J.P., Asymptotic analysis of Bloch-Floquet waves in a thin bi-material strip with a periodic array of finite-length cracks, Waves Random Complex Media, 17 (2007) 511-533.
[7] Vellender, A., Mishuris, G.S., Movchan, A.B., Weight function in a bimaterial strip containing an interfacial crack and an imperfect interface. Application to Bloch-Floquet analysis in a thin inhomogeneous structure with cracks, Multiscale Model. Simul., 9 (2011) 1327-1349.
[8] Vellender, A., Mishuris, G.S., Eigenfrequency correction of Bloch-Floquet waves in a thin periodic bi-material strip with cracks lying on perfect and imperfect interfaces, Wave Motion, 49 (2012) 258-270.
[9] Zalipaev, V.V., Movchan, A.B., Jones, I.S., Two-parameter asymptotic approximations in the analysis of a thin solid fixed on a small part of its boundary, Q. J. Mech. Appl. Math., 60 (2007) 457-471.
[10] Gei, M., Jones, I.S., Movchan, A.B., Junction conditions for cracked elastic thin solids under bending and shear, Q. J. Mech. Appl. Math., 62 (2009) 481-493.
[11] Carta, G., Brun, M., Movchan, A.B., Dynamic response and localization in strongly damaged waveguides, Proc. R. Soc. A, 470 (2014) 20140136.
[12] Dimarogonas, A.D., Vibration of cracked structures: A state of the art review, Eng. Fract. Mech., 55 (1996) 831-857.
[13] Ostachowicz, W.M., Krawczuk, M., Analysis of the effect of cracks on the natural frequencies of a cantilever beam, J. Sound Vib., 150 (1991) 191–201.
[14] Chondros, T.G., Dimarogonas, A.D., Yao, J., Vibration of a beam with a breathing crack, J. Sound Vib., 239 (2001) 57-67.
[15] Mead, D.J., Wave propagation and natural modes in periodic systems: I. Mono-coupled systems, J. Sound Vib., 40 (1975) 1–18.
[16] Brun, M., Giaccu, G.F., Movchan, A.B., Movchan, N.V., Asymptotics of eigenfrequencies in the dynamic response of elongated multi-structures, Proc. R. Soc. A, 468 (2012) 378-394.
[17] Ciarlet, P.G., Mathematical Elasticity Volume II: Theory of Plates, first ed., North-Holland, Amsterdam, (1997).
[18] Pestel, E.C., Leckie, F.A., Matrix methods in elastomechanics, first ed., McGraw-Hill, New York, (1963).
[19] Faulkner, M.G., Hong, D.P., Free vibrations of mono-coupled periodic system, J. Sound Vib., 99 (1985) 29–42.
[20] Lekner, J., Light in periodically stratified media, J. Opt. Soc. Am. A, 11 (1994) 2892–2899.
[21] Romeo, F., Luongo, A., Invariants representation of propagation properties for bi-coupled periodic structures, J. Sound Vib., 257 (2002) 869–886.